Circle Detection in Pulsative Medical Video Sequence

Kamil Říha, Radek Beneš
Department of Telecommunications
Brno University of Technology
Purkyňova 118, 612 00 Brno
CZECH REPUBLIC
e-mail: rihak@feec.vutbr.cz, xbenes30@ stud.feec.vutbr.cz

***Abstract*— the article deals with a new method for the detection of pulsative circular objects in a medical video sequence. The motivation for investigating this method consists in the fact that a circular object is not very apparent and its detection in such a frame is inaccurate. In some cases of medical images, the pulsative character of the circular area being searched can be used for its localisation. The proposed method starts from an analysis of movement, using optical flow estimation. The compensation of global movement is necessary because only local pulsative movement during the video sequence is assumed. The optical flow estimation is followed by another main processing step: the Hough Transform for the circle position estimation. Circles with expected properties are selected using the Bayes classifier. Finally, the circle position in a single frame is adapted using the analysis of average pixel intensity in the directions starting from the circle centre.**

Keywords-Circle detection, Video sequence, Optical flow, Hough Transform, Bayes classifyer

I. INTRODUCTION

The circular pattern detection in digital images is the one of the basic tasks of the digital image processing. Manny approaches have been proposed for this purpose. The best known and the most used is the Circle Hough Transformation (CHT) [1], [2]. This method mostly uses the edge image and searches the circle both with known and unknown radius. Circular pattern can be also localised using correlation [3], maximal likelihood [4] or the symmetry of the gradient field methods [5]. Recently, the using of genetic algorithms is tested for solving the problem [6], [7] (computationally expensive).

Above mentioned techniques are used mainly in situations, where the circle is searched in a single frame. Nevertheless, there exist situations, when a number of frames are available containing a dynamic circular pattern. Based on this fact, the information from this number of frames can be used in the process of a circle localisation. The concrete example of a pulsing circle object is the artery (*carotis communis*) perpendicular cut captured by sonograph. The displayed artery cut is approximately circular shaped with dynamic radius. The artery wall can be seen in single frames as a bright areas (see Fig. 3(a)). Single arbitrary image of an artery can be used for the localisation directly using one of some above mentioned methods, but the artery wall is not sufficiently perceptible and so these methods are often unsuccessful. Hence, methods for utilisation of the movement of the circular carotid area have been researched. This article presents such a new complex method using the Horn & Shunck technique [8] for the movement analysis between each pair of two consequential frames. After the optical flow technique application, the resulting movement fields are averaged and rectified for the Hough Transform.

II. THE CIRCLE DETECTION PROCEDURE

The procedure can be divided to tree consequential steps: source frames preprocessing, circular pattern localisation and exact radius determination (see Fig. 1).

The principle of ultrasound sequence acquisition consists in "free hand" probe manipulation, and due to this fact the record is often degraded by a global motion. This motion could impair the results of the optical flow analysis, so maximum effort is taken to eliminate it by using motion compensation [9]. After this preprocessing, there is mainly the pulsative movement and the less important movements (caused by minor movements of the other tissue) in the image. The preprocessing block also contains the common Gaussian filter for noise removal [10].

A. Circular Pattern Localisation

The basic idea of the localisation follows from the hypothesis that there is no other meaningful movement, with the exception of the pulsative movement of the circular pattern. There are common minor movements, for example the muscular movement caused by patient discomposure during the acquisition. However, these movements are short-lived and they will not be apparent in the results, due to averaging (see the following text for details) in a long video sequence. At first, each pair of consecutive frames is analyzed and the optical flow is determined. Using the Horn & Schunck method, Ndense motion fields $\vec{u}_n(i,j)$ are generated – one for each of n-th pair of consecutive frames. With a view to reducing the computational cost of the proposed algorithm, only the absolute values of motion vectors are taken into account in the following steps, which are calculated using the following equation

$$v_n(i,j) = \|\vec{u}_n(i,j)\| \cong x_n^2(i,j) + y_n^2(i,j). \qquad (1)$$

Manuscript received May 27, 2010. This work was prepared with the support of the MSMT projects No. 2B06111 and MSM 0021630513.

R. Beneš is with the Faculty of Electrical Engineering and Communication, Brno University of Technology, Udolni 244/53, CZ-60200 Brno, Czech Republic (e-mail: xbenes30@ stud.feec.vutbr.cz).

K. Říha is with the Faculty of Electrical Engineering and Communication, Brno University of Technology, Udolni 244/53, CZ-60200 Brno, Czech Republic (e-mail: rihak@feec.vutbr.cz).

978-1-4244-5899-8/10/$26.00 ©2010 IEEE

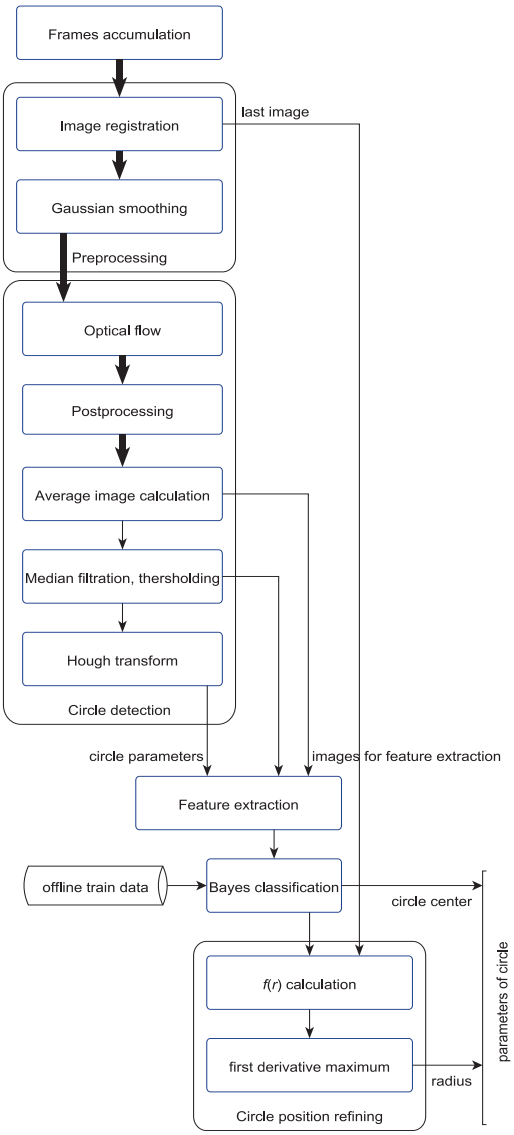

Figure 1. Block diagram of the complete method

Moreover, the vector norms are recalculated to emphasize the more significant movements by the exponential function and to suppress less significant movements via thresholding, using the equation

$$v'_n(i,j) = \begin{cases} 0 & \text{if } v_n(i,j) \leq 1 \\ e^{v_n(i,j)} & \text{if } v_n(i,j) > 1 \end{cases}. \qquad (2)$$

Equations (1) and (2) represent the recalculation of all the vectors $\vec{u}_n(i,j)$ in all N vector fields with the result of N scalar fields $v'_n(i,j)$. Partial fields represent the evaluation of movement in every image element. The next step is the averaging of these N scalar fields, using the equation

$$k(i,j) = \frac{v'_0(i,j) + v'_1(i,j) + \cdots + v'_{N-1}(i,j)}{N}. \qquad (3)$$

The scalar field of elements $k(i,j)$ has the same size as the input frames and represents the average evaluation of the movement in $N+1$ consecutive frames. The resulting field can be taken as an image where the bright values mean more significant movement (see Fig. 3(b)). The scalar field of elements $k(i,j)$in the form given in Fig. 3(b) is not suitable for a direct application of the Hough Transform and therefore some morphological processing steps are used for its modification. The steps are:

- dilation using elliptic convolution kernel (the result can be seen in Fig. 3(c)),
- thresholding that transforms image data into binary field (the result can be seen in Fig. 3(d) where white elements denote areas with sufficient movement and the black ones mean areas without sufficient movement),
- median filtering (with the 19 × 19 kernel) for spatial "smoothing" of the binary filed,
- conversion from the binary image (see Fig. 3(e)) to the edge image and finally
- application of the Circle Hough Transform.

The Hough Transform represents a conversion from 2D edge image (geometrical space) to 3D Hough parametrical space of the circle parameters being sought (x_s, y_s, r), where x_s, y_s are circle centre coordinates and r denotes its radius). The transformation itself starts from the analytic circle description

$$\begin{aligned} x &= x_s + r \cdot \cos(\phi) \\ y &= y_s + r \cdot \cos(\phi) \end{aligned}, \qquad (4)$$

where $\phi \in \langle 0, 2\pi \rangle$.

The analytic representation of circle is used for the construction of so-called accumulator, or the Hough space, where some maximums can be found whose coordinates represent the parameters of the most probable circles. The Hough Transform is very tolerant to contour interruption. On the other hand, there is a disadvantage resulting from the following: more potential circles can be found in places where there are no relevant objects to be detected. A single parameterized circle is expected as the result, and due to this fact a single circle has to be chosen in a set of maximal values in the parametric space. The simplest way is to choose the circle which is represented by the maximum in the Hough parametric space. However, this maximum need not be the representation of the correct circle, which means a smaller detection reliability. Due to this, the prior knowledge of pixel parameters localised inside the detected circle is used for the improvement of the detection reliability. The prior information is used to train the Bayes [10].

A number of most probable circles in the parametric space are then processed by the Bayes classifier with the goal to choose the best circle. The feature vector for the classifier consists of statistic values acquired from the pixel intensity localised inside the manually denoted circles from the training

data set (average value and standard deviation). Similar features are obtained for a circle of smaller radius and for a circle from binary image.

A concrete implementation of the normal Bayes classifier supposes a normal distribution of feature vectors. The average value and covariance matrix are calculated for every class and the following classification is executed based on this information. The classification is trained by the feature vector for executing the selection into two classes: the first represents circles with the properties being sought, and the second represents the rest. In this way, the most probable artery circle is selected from a number of potential circles.

B. Determination of Exact Radius

Up to this point, the sequence of (approx. 20-50, in dependence on user settings) frames has been processed. The number of frames is chosen as a compromise between the time needed for the accumulation of frames to a buffer and the required accuracy (more frames mean greater accuracy but also more time for computation, see the section Experimental Results). The captured circle is pulsating, but its centre is in stable position during the video sequence. Hence, the circle centre is determined accurately but the radius is calculated approximately as an average value of all the radiuses in the video sequence.

For the following process, the exact value of the radius in a frame is needed. The frame for this step is mostly the last one, because this frame could be the starting point for subsequent processing in the real-time version. The specification of circle radius uses the knowledge of the centre position and of the average value of radius r_{act}. Let us consider the range of radiuses $\langle 0.5 \cdot r_{act}, 1.5 \cdot r_{act} \rangle$. This range has been chosen empirically so that the arterial wall area is safely selected. The radius being sought is in the specified range and so the calculation of the exact arterial wall position can be restricted to this range. The intensities of image pixels are analysed inside the ring-shaped area with the radius r (see Fig. 2(a)). Concretely, the average value of image elements localised inside the area is analysed. This average value depends on the radius of the ring (see Fig. 2(b)).

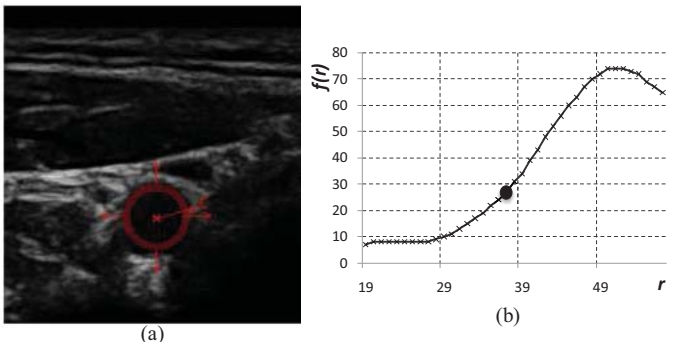

(a) (b)

Figure 2. (a) Processed image with the denoted ring area where the pixels are analyzed, (b) $f(r)$ curve describing the dependence of average intensity in the ring area with respect to the radius r.

The circle border is brighter than the inner part of an artery, that is why the average intensity is increasing with the value of the radius. If the ring size is larger, then the average intensity declines.

The above-described behaviour of the function $f(r)$ implies, that the artery border can be detected as a part of the curve with the highest 1-st derivative (the part of the curve with the largest increment, denoted in Fig. 2(a)). The radius coordinate of this curve part can be calculated as

$$r_k = \arg\max_r \left(\frac{\Delta f(r)}{\Delta r} \right). \quad (5)$$

The parameters of detected circle (x_s, y_s, r_k) are now available, which means the final result of the process.

III. Experimental Results

A. Detection Accuracy

The proposed method has been tested on a set of 250 video sequences. This set has been acquired by the examination of a few test persons, with differently set-up sonographic device and with different rates of global movement (translation movement of the probe). Such a testing set (denoted *real test set (set A)*) is a representation of test data acquired in real conditions. There are many low quality sequences in this test set, with image noise or (and) with a high level of global movement. These factors will cause a decrease in the method reliability.

The proposed method was also tested on a second test set, which is a subset of the original test set and does not include sequences that are affected by global translational motion. This test set will be referred to as *test set without motion (set B)*. Such sequences should be processed if the acquisition is without undesirable movement.

The circle detection accuracy (see TABLE I) was evaluated visually. If the circle was detected, its precise position was in most cases sufficient. Only in certain cases was the localization slightly imprecise (position or radius of the circle was not correct) and in such cases the detection was counted as unsuccessful.

B. Time Complexity

Time complexity of the proposed method increases linearly with the total number of frames in the video sequence, because most processing steps are applied to each pair of consecutive frames. With the hardware used (Intel Core 2 Duo E8400, 3GHz), the processing of forty frames takes from 2.6 to 3.2s (processing time also depends on the data). The main part of this time is used to calculate the optical flow and motion compensation in input images.

If the proposed method works with the data being captured in real-time, the extra time needed for accumulating the required number of frames to buffer must be taken into consideration. This extra time will occur in the processing as a constant delay, which depends on the length of the processed video sequence and frame rate.

TABLE I. DETECTION RELIABILITY AND COMPUTATIONAL COST

Number of processed frames	***Reliability (set A)***	***Reliability (set B)***	***Average period of computation***
20	78.1 %	82.1 %	1730 ms
30	79.2 %	83.7 %	2300 ms
40	82.5 %	85.1 %	2950 ms
50	83.0 %	85.1 %	3720 ms

CONCLUSION

A novel method for the detection of pulsating circles in medical video sequences has been presented. The method analyses the pulsative movements in the source sequence with the aim to improve the reliability in comparison with methods using a static images.

The proposed method also achieves good results on the set of sequences containing complication factors (inconsistent shapes, movement of image, noise, etc.). It can be seen from the results that the longer the sequence (more images in sequence) used, the higher the accuracy achieved. This stems from the fact that some minority movements, which generate nonzero optical flow even in places beyond the pulsating movement, are suppressed in longer sequences thanks to the averaging of optical flow. A greater number of initialization images has also some drawbacks: the time required to accumulate the number of initialization images is higher and also the processing of accumulated images is more time-consuming. The increase in accuracy is not exactly linear (see TABLE I) and therefore the utilization of longer initialization sequences has not resulted in further significant increases in success.

REFERENCES

[1] R. O. Duda and P. E. Hart, "Use of the Hough Transformation to detect lines and curves in pictures," *Commun. ACM*, vol. 15, no. 1, pp. 11–15, 1972. [Online]. Available: http://doi.acm.org/10.1145/361237.361242

[2] T. J. Atherton and D. J. Kerbyson, "Size invariant circle detection," *Image and Vision Computing*, vol. 17, no. 11, pp. 795 – 803, 1999. [Online]. Available: http://www.sciencedirect.com/science/article/B6V09-3X5368N-2/2/f5d2964d9228a494aaa65f2adc7a745e

[3] M. Ceccarelli, A. Petrosino, and G. Laccetti, "Circle detection based on orientation matching," in *11th International Conference on Image Analysis and Processing (ICIAP'01)*, vol. 0, p. 0119, 2001.

[4] I. Frosio and N. A. Borghese, "Real-time accurate circle fitting with occlusions," *Pattern Recogn.*, vol. 41, no. 3, pp. 1041–1055, 2008.

[5] A. A. Rad, K. Faez, and N. Qaragozlou, "Fast circle detection using gradient pair vectors," in *VIIth Digital Image Computing: Techniques and Applications*, 2003, pp. 879–887.

[6] V. Ayala-Ramirez, C. H. Garcia-Capulin, A. Perez-Garcia, and R. E. Sanchez-Yanez, "Circle detection on images using genetic algorithms," *Pattern Recognition Letters*, vol. 27, no. 6, pp. 652 – 657, 2006. [Online]. Available: http://www.sciencedirect.com/science/article/B6V15-4HNSFXX-1/2/847b3ba2986c4ecf351990dc28703250

[7] G. Roth and M. Levine, "Geometric primitive extraction using a genetic algorithm," in IEEE Transactions on Pattern Analysis and Machine Intelligence, vol. 16, no. 9, pp. 901–905, September 1994.

[8] B. K. Horn and B. G. Schunck, *Determining optical flow,* Tech. Rep., Cambridge, MA, USA, 1980.

[9] H.-W. C. M. Chang, J.Y. and B. Chang, "Digital image translational and rotational motion stabilization using optical flow technique," in *IEEE Transactions on Consumer Electronics*, vol. 48, no. 1, pp. 108–115, 2002.

[10] K. Fukunaga, *Introduction to statistical pattern recognition (2nd ed.)*. San Diego, CA, USA: Academic Press Professional, Inc., 1990.

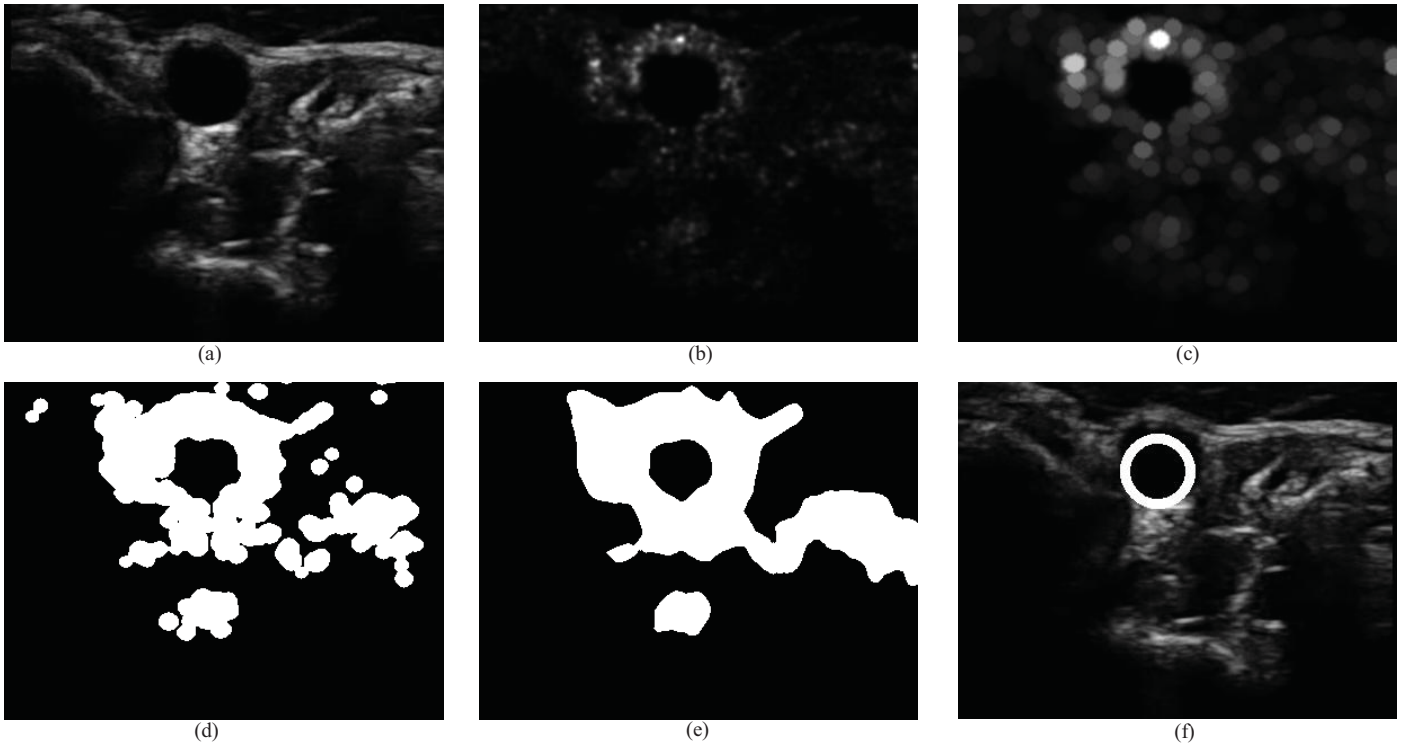

Figure 3. Images of the consecutive processing steps for the circle localisation: (a) single frame example from the source video sequence, (b) scalar field of elements $k(i,j)$ (the average of the vector field absolute values), (c) visualised data after the dilation step, (d) thresholded image, (e) visualised data after the median filtering step, (f) visualised data after the Hough Transform step.